

## Supporting Information

# Synthesis and Upconversion Luminescence of $\text{BaY}_2\text{F}_8:\text{Yb}^{3+}/\text{Er}^{3+}$ Nanobelts

Guofeng Wang, Qing Peng, and Yadong Li\*

*Department of Chemistry and State Key Laboratory of New Ceramics and Fine Processing, Tsinghua University, Beijing, 100084 (P. R. China)*

### 1. Experimental details

Chemicals: Analytical grade  $\text{Y}_2\text{O}_3$ ,  $\text{Yb}_2\text{O}_3$ ,  $\text{Er}_2\text{O}_3$ , NaF,  $\text{BaCl}_2$ , hydrochloric acid (HCl), cyclohexane, ethanol, and oleic acid were obtained from Beijing Chemical Reagents, China. All of the reagents and solvents were used as received without further purification. Deionized water was used throughout.  $\text{Y}_2\text{O}_3$ ,  $\text{Yb}_2\text{O}_3$ , and  $\text{Er}_2\text{O}_3$  were separately dissolved in dilute HCl by heating to prepare the stock solutions of  $\text{YCl}_3$ ,  $\text{YbCl}_3$ , and  $\text{ErCl}_3$ .

$\text{BaY}_2\text{F}_8:\text{Yb}^{3+}/\text{Er}^{3+}$  nanobelts were obtained as follows: 20 ml oleic acid, 1.2 g NaOH, 8 ml alcohol, 5 ml deionized water were mixed together, to which 0.25 mmol of chloride salts ( $\text{BaCl}_2$ ,  $\text{YCl}_3$ ,  $\text{YbCl}_3$ , and  $\text{ErCl}_3$ ) aqueous solution and 4 mL of sodium fluoride solution (0.5 mol/L) were then added under vigorous stirring. Subsequently, the milky colloidal solution was transferred to a 50 mL Teflon-lined autoclave, and heated at 200 °C for 24 h. The systems were then allowed to cool to room temperature. The final products were collected by means of centrifugation, washed with ethanol, and then dried under vacuum at 80 °C.

Characterization: The crystal structure was analyzed by a Rigaku RU-200b X-ray powder diffractometer (XRD) using a nickel-filtered Cu K $\alpha$  radiation ( $\lambda = 1.5418 \text{ \AA}$ ). The size and morphology of the final products were determined by using JSM-6301F scanning electron microscope (SEM) and JEOL JEM-2010F transmission electron microscope operated at 200 kV.

UC luminescence spectra were recorded using a Hitachi F-4500 fluorescence spectrophotometer with an adjustable laser (980 nm) as the excitation source with a fiber-optic accessory.

### 2. Power dependence of UC luminescence

Figure S3a shows the intensity ratio of  ${}^2\text{H}_{11/2}/{}^4\text{S}_{3/2} \rightarrow {}^4\text{I}_{15/2}$  to  ${}^4\text{F}_{9/2} \rightarrow {}^4\text{I}_{15/2}$  as a function of excitation power density in  $\text{BaY}_2\text{F}_8:\text{Yb}^{3+}/\text{Er}^{3+}$  (40/4) nanobelts. We can see that the emission ratio increased with increasing excitation power density. It is reasonable to ascribe this to the three-photon UC luminescence phenomenon for the green levels. Similar behavior has also been observed in  $\text{CaF}_2:\text{Yb}^{3+}/\text{Er}^{3+}$  nanocrystals.<sup>1</sup> In addition, the relative intensity of  ${}^2\text{H}_{11/2} \rightarrow {}^4\text{I}_{15/2}$  to  ${}^4\text{S}_{3/2} \rightarrow {}^4\text{I}_{15/2}$  also increased with increasing excitation power density, which can be attributed to thermal effects (Figure S3b).<sup>2</sup>

### Reference for the supporting information

1. G. Wang, Q. Peng and Y. Li, *J. Am. Chem. Soc.*, 2009, **131**, 14200-14201.

- 2.** X. Bai, H. Song, G. Pan, Y. Lei, T. Wang, X. Ren, S. Lu, B. Dong, Q. Dai and L. Fan, *J. Phys. Chem. C*, 2007, **111**, 13611-13617.

**Figure S1.** (a,b) SEM and (c) TEM images of  $\text{BaY}_2\text{F}_8:\text{Yb}^{3+}/\text{Er}^{3+}$  (40/4) nanobelts.

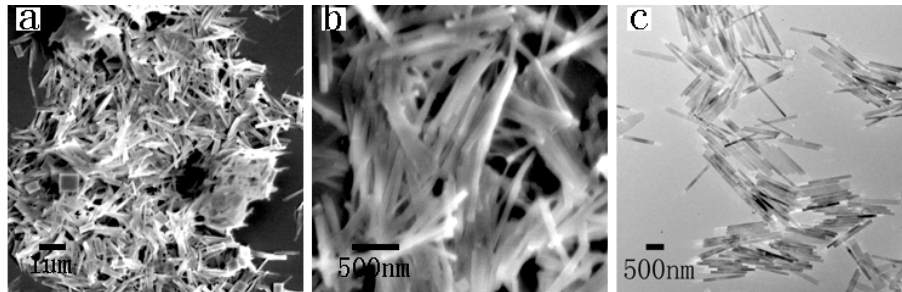


**Figure S2.** Energy-level and UC schemes for the  $\text{Yb}^{3+}\text{-Er}^{3+}$  system.

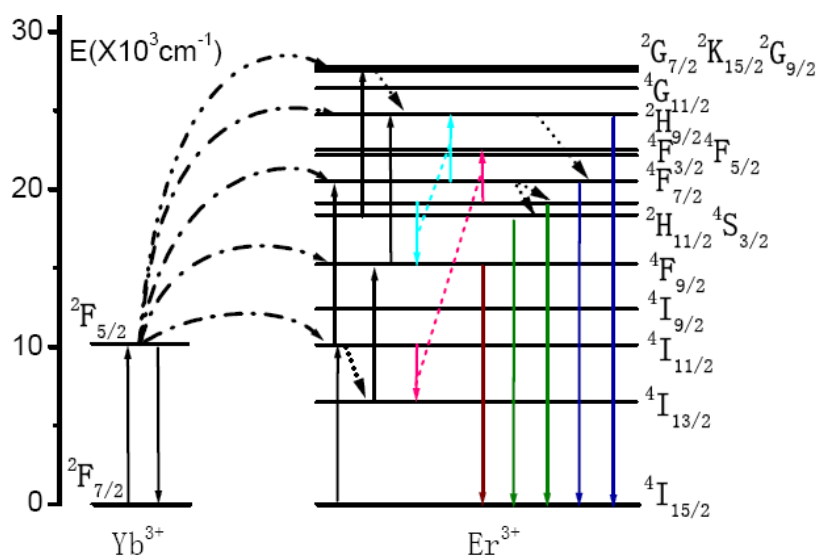


**Figure S3.** (a) The intensity ratio of  ${}^2H_{11/2}/{}^4S_{3/2} \rightarrow {}^4I_{15/2}$  to  ${}^4F_{9/2} \rightarrow {}^4I_{15/2}$  as a function of excitation power. (b) The intensity ratio of  ${}^2H_{11/2} \rightarrow {}^4I_{15/2}$  to  ${}^4S_{3/2} \rightarrow {}^4I_{15/2}$  as a function of excitation power.

